

Taylor Predictor Improves Chaos Controller

Arūnas Tamaševičius, Elena Tamaševičiūtė, Gytis Mykolaitis, and Skaidra Bumeliene

Abstract— Chaos controllers used for stabilizing unstable periodic orbits and/or unstable steady states are very sensitive to unavoidable latency of the controlling feedback force. When the delay value exceeds some critical value the controller fails to work. We consider a specific case of a derivative control applied to stabilize unstable steady state in a third-order autonomous chaotic oscillator. We demonstrate from equations, by PSPICE simulations, and hardware experiments that inserting in the feedback control loop the Taylor predictor essentially improves the performance of the controller.

I. INTRODUCTION

Control of chaotic behaviors in dynamical systems has become one of the most rapidly developing topics in nonlinear science and engineering in the last two decades. Most investigations in the field of controlling chaos deal with stabilization of unstable periodic orbits embedded in chaotic attractors [1, 2]. Along with unstable periodic orbits any autonomous chaotic system contains at least one unstable steady state (USS) that can also be stabilized by various feedback techniques [3-9]. Most simple is the derivative control technique [3-5], successfully applied to lasers [3], electrical circuits [4] and electrochemical reactions [5]. More sophisticated is the delayed feedback method [6-9]. The latter has been employed to stabilize steady states in electrical circuits [6, 7] and electrochemical systems [8, 9]. A serious limitation of the feedback methods is the additional time lag in the control loops [10-12], especially in fast experimental systems. Latency decreases the range of feedback gains over which control is achieved. Eventually longer latency times can totally destroy the control algorithm. To overcome the latency problem a straightforward solution is to insert in the feedback loop a time lead device that compensates time lag effects. In the context of broadband and fast chaotic systems the Taylor type analogue predictors [13-15] are very promising. In the present paper we consider an extremely simple first-order Taylor predictor used to assist the derivative controller, which is intended to stabilize unstable steady state in a chaotic circuit.

II. CHAOTIC SYSTEM

We consider extremely simple third-order autonomous chaotic oscillator, the so-called Vilnius chaotic oscillator [16], described in details elsewhere [17-19]. Though intended as a training tool for students the oscillator due to its simplicity seems to be a convenient circuit for demonstrating various techniques of chaos control.

E.T. was partially supported by the Gifted Student Fund—Lithuania. All the authors are with the Plasma Phenomena and Chaos Laboratory, Semiconductor Physics Institute, Vilnius, Lithuania, LT-01108; E.T. is also with the Department of Radiophysics, Vilnius University. E-mail: tamasev@pfi.lt, elena.tamaseviciute@ff.vu.lt

The circuit diagram of the oscillator and the chaotic phase portrait are shown in Fig. 1 and Fig. 2, respectively. The oscillator includes three inertial elements ($L1$, $C1$, and $C2$), one nonlinear device (diode D), and a single OA1 based amplifying stage. An auxiliary unit is the current source I_0 used to set the dc bias of the diode D . The voltage across the R (also the output voltage of the OA1), the voltage across $C1$, and the voltage across $C2$ can be taken as the output of the oscillator. High frequency implementation of the oscillator using fast Schottky diodes is discussed in [20].

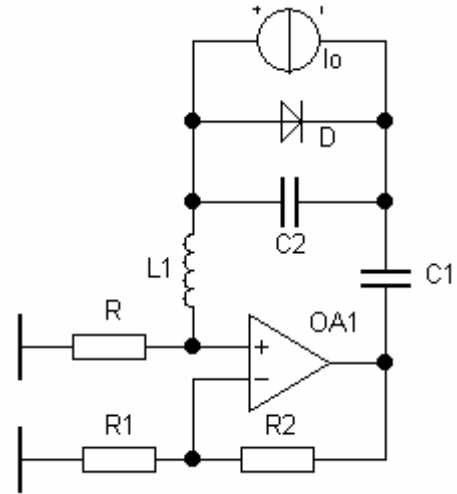


Fig. 1. Circuit diagram of the oscillator. $L1 = 1 \mu\text{H}$, $C1 = 100 \text{ pF}$; fundamental frequency $f^* = 1/2\pi(L1C1)^{1/2} \approx 16 \text{ MHz}$, surge impedance $Z = (L1/C1)^{1/2} = 100 \Omega$. $C2 = 15 \text{ pF}$, $R = 100 \Omega$, $R1 = 10 \text{ k}\Omega$, $R2 = 6.8 \text{ k}\Omega$ (trimmer-pot). Open-loop gain $\gamma_1 = R2/R1 + 1$.

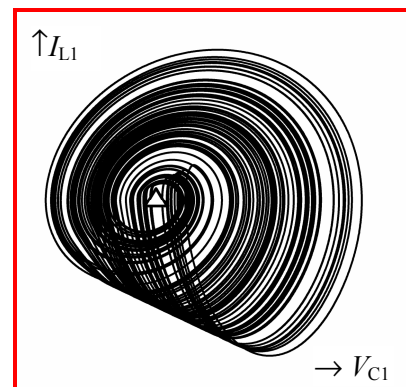


Fig. 2. Phase portrait from the chaotic oscillator. Current I_{L1} has been taken as a voltage drop across grounded resistor R , voltage V_{C1} has been taken via differential amplifier (not shown in the diagram). $I_0 = 7.5 \text{ mA}$, $R2 = 4 \text{ k}\Omega$ ($\gamma_1 = 1.4$). Triangle in the center of the attractor marks unstable steady state ($V_{C1} \approx -0.4 \text{ V}$, $I_{L1} = 0$).

III. MATHEMATICAL MODEL

The oscillator in Fig. 1 is described by a set of three ordinary differential equations [17, 19]:

$$\begin{aligned}\dot{x} &= y, \\ \dot{y} &= -x + ay - z, \\ \varepsilon \dot{z} &= b + y - c(\exp z - 1).\end{aligned}\quad (1)$$

It has a non-zero USS:

$$x_o = -\ln\left(\frac{b}{c} + 1\right) < 0, \quad y_0 = 0, \quad z_0 = \ln\left(\frac{b}{c} + 1\right) > 0. \quad (2)$$

Let us apply the control via the equation for 'y':

$$\begin{aligned}\dot{x} &= y, \\ \dot{y} &= -x + ay - Q_N, \\ \varepsilon \dot{z} &= b + y - c(\exp z - 1).\end{aligned}\quad (3)$$

Here Q_N is the control term; $N=1, 2$, or 3 depends on the specific control scheme, i.e. (a), (b), or (c) in Fig. 3. Solution (2) is an unstable point and it is just the goal of the controller. In this paper we consider the derivative control algorithm given by

$$Q_1(t) = k\dot{x}. \quad (4)$$

Here k is the feedback coefficient. For the specific system, given by (1), the derivative in (4) can be replaced by 'y':

$$Q_1(t) = ky. \quad (5)$$

Then it is evident that for $k > a$ the overall system is a damped system and the USS (2) becomes globally stable. The control term $Q_1(t)$ asymptotically vanishes when the system approaches (x_0, y_0, z_0) . The numerical results including the uncontrolled stage, the transients and the goal steady state are illustrated in Fig. 4. The variable $x(t)$ converges, as expected, to its non-zero state $x_0 = -22.7$ (for $b = 30, c = 4 \times 10^{-9}$); the control term $Q_1(t)$ after a short transient reduces to zero.

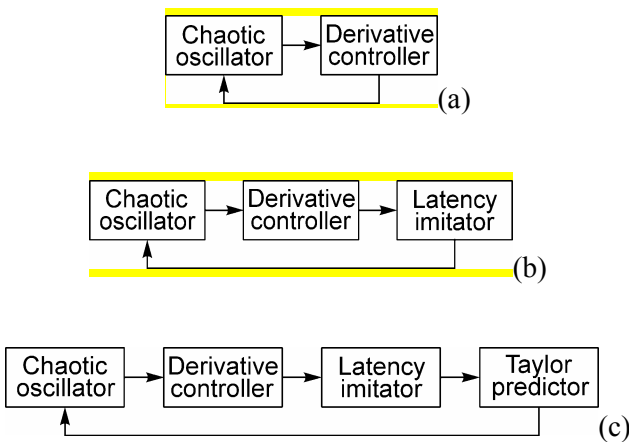


Fig. 3. Block diagrams of the control setup. (a) ideal control, (b) control with parasitic latency, (c) control with latency compensated by means of the Taylor predictor.

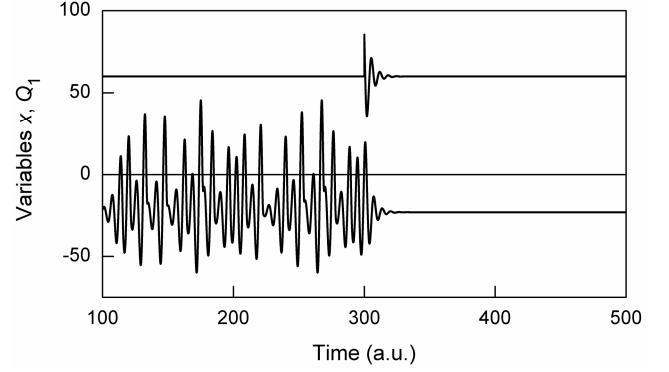


Fig. 4. Numerical results from (3) with the control term Q_1 . $k = 0.8$. Other parameters $a = 0.4, b = 30, c = 4 \times 10^{-9}, \varepsilon = 0.13$. Lower trace is variable $x(t)$. Upper trace is the control signal Q_1 (the latter is arbitrarily shifted up by 60 from zero level for clarity). Control is activated at $t = 300$.

To imitate the latency we employ the first-order circuit, specifically a low-pass RC filter. There are three motivation points behind such a choice. Firstly, the R imitates loss effects in a real circuit and the capacitor C represents parasitic mounting capacitance. Secondly, the filter is characterized by a constant unity gain and a constant delay time $T_{\text{del}} \approx RC$ at lower frequencies, also by rather natural falloff of the gain (minus 6 decibels per octave) at higher frequencies. Thirdly, the mathematics is extremely simple:

$$hu = Q_1 - u, \quad (6)$$

where parameter h is the normalized dimensionless latency. The output signal of the filter u is just the control term: $Q_2(t) = u$. For $h = 0, Q_2 = Q_1$, as expected. At low frequencies $Q_2(t) \approx Q_1(t-h)$. Numerical results with Q_2 applied to (3) are presented in Fig. 4b. In contrast to the previous case the controller with latency fails to stabilize the USS. Moreover, it raises high frequency undesired oscillations.

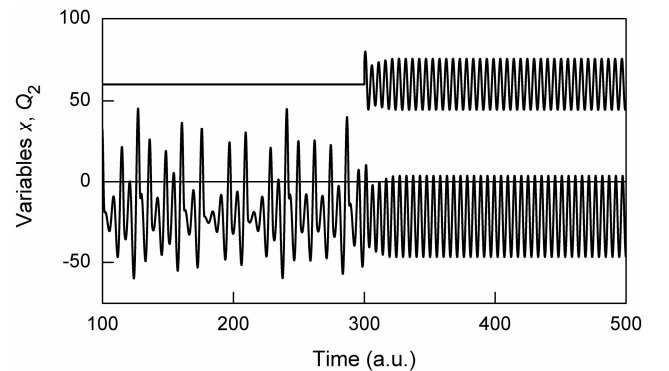


Fig. 5. Numerical results from (3) with the control term Q_2 . $h = 1$. Other parameters and layouts are the same as in Fig. 4.

To compensate the latency we suggest inserting in the control loop the first-order Taylor predictor. Then the control signal reads

$$Q_3(t) \approx Q_2(t+g) \approx u + gu = u + (g/h)(Q_1 - u). \quad (7)$$

The following approximate relation between Q_3 , Q_2 , and Q_1 is valid at lower frequencies

$$Q_3(t) \approx Q_2(t+g) \approx Q_1(t-h+g). \quad (8)$$

We note that g in (8) should not necessarily equal h . However, when this is the case both (8) and (9) read: $Q_3(t) \approx Q_1(t)$. So, the compensating effect of the predictor becomes very clear. Numerical results are shown in Fig. 6 for Q_3 described by (8) with $g=h$. They do confirm perfect performance of the improved controller.

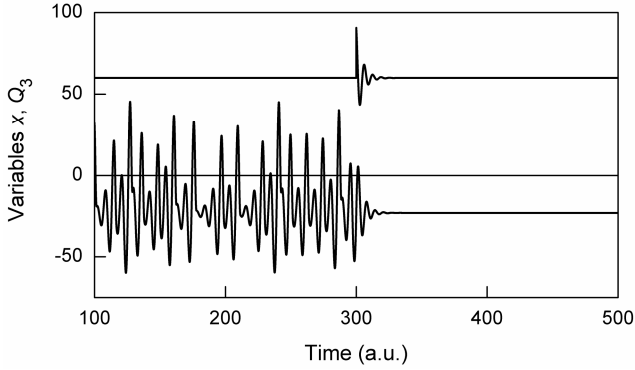


Fig. 6. Numerical results from (3) with the control terms Q_3 . $h = g = 1$. Other parameters and layouts are the same as in Fig. 4.

Let us consider now more complicated and more realistic latency unit introduced by an RLC low-pass filter, where L imitates parasitic wiring inductance. The dimensionless equations read

$$\begin{aligned} h\dot{v} &= Q_1 - u - v, \\ h\dot{u} &= v. \end{aligned} \quad (9)$$

Here the output variable is u . So the control signal with latency is $Q_2(t) = u$. The effective latency time for the RLC filter is $h_{eff} = \sqrt{2}h$ at the same threshold frequency as for the RC filter, considered before. Therefore, the parameter h in (9) should be diminished by a factor of $\sqrt{2}$ (see caption to Fig. 7) to have the same latency time as for the RC filter.

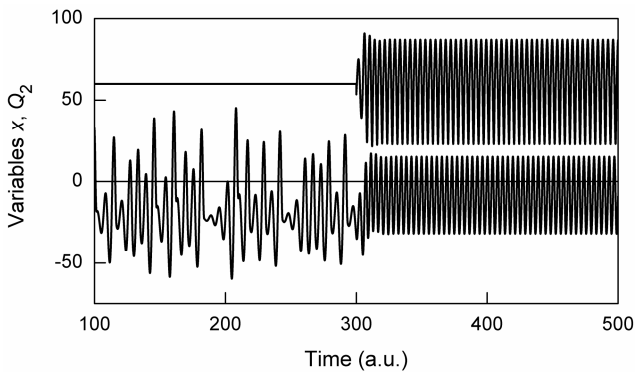


Fig. 7. Numerical results from (3) with the control term $Q_2(t) = u$ from (9). $h = 0.71$. Other parameters and layouts are the same as in Fig. 4.

Correspondingly the control signal with prediction is

$$Q_3(t) \approx Q_2(t+g) \approx u + g\dot{u} = u + (g/h)v. \quad (10)$$

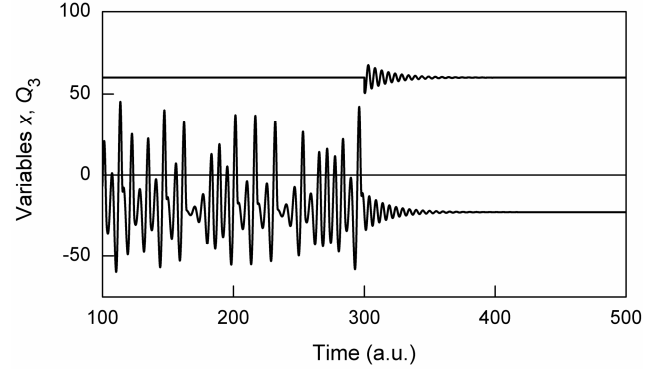


Fig. 8. Numerical results from (3) with the control term $Q_3(t)$ from (10). $h = 0.71$, $g = 1$. Other parameters and layouts are the same as in Fig. 4.

IV. ANALOGUE CIRCUITS

All the blocks in Fig. 3 have been implemented by means of analogue components. The corresponding circuit diagrams are shown in Fig. 9 through Fig. 13. As discussed in Section III the oscillator has unstable non-zero steady state. By setting $L1$, $C1$, and $C2$ values the oscillator has been tuned to operate in a megahertz frequency band [20]. The diode D in Fig. 9 is low junction capacitance (≈ 1 pF) fast recovery (≈ 10 ps) BAT68 Schottky device; $I_0 = 7.5$ mA. All the operational amplifiers from OA1 to OA9 are the HFA-002 ($f_{th} = 1$ GHz) type chips. Other circuit parameter values and necessary comments are given in the specific figure captions.

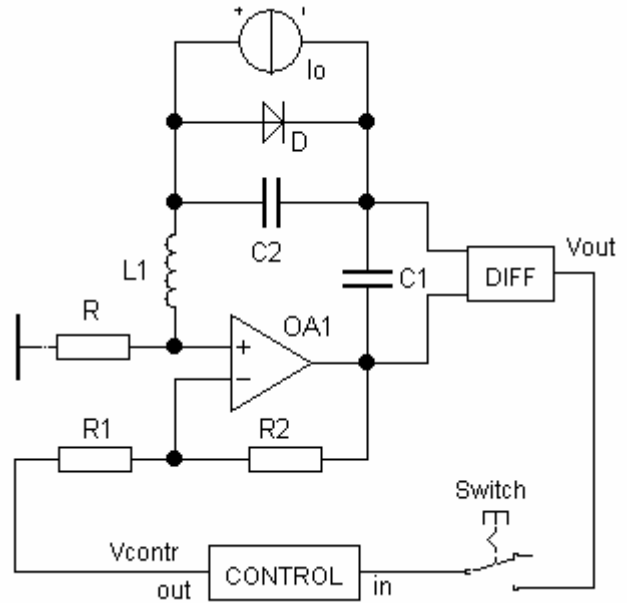


Fig. 9. Controlled oscillator. Circuit parameters of the oscillator are the same as in Fig. 1. DIFF is a differential amplifier; $V_{out} = V_{C1}$. Circuit diagram of the CONTROL unit is shown in Fig. 10.

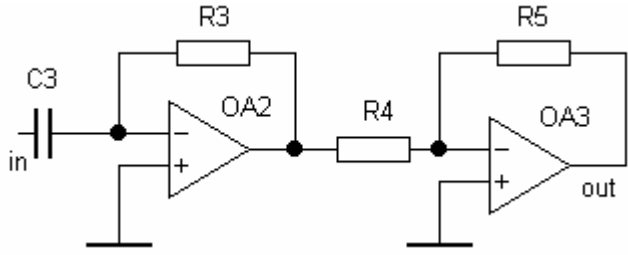


Fig. 10. CONTROL unit (a derivative controller). OA2 stage is a differentiator. $V_{out} = R3C3 \times dV_{in}/dt$. $R3C3 = (L1C1)^{1/2}$. OA3 stage is an inverter. $R4 = R5 = 1 \text{ k}\Omega$.

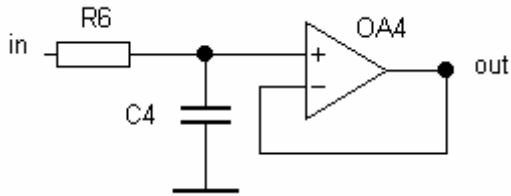


Fig. 11. RC latency imitator. $R6 = 100 \Omega$, $C4 = 100 \text{ pF}$. $T_{del} \approx R6C4 = 10 \text{ ns}$. OA4 stage is a buffer.

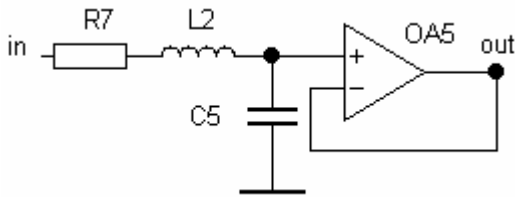


Fig. 12. RLC latency imitator. $R7 = 150 \Omega$, $L2 = 0.7 \mu\text{H}$, $C5 = 68 \text{ pF}$. $T_{del} \approx (2L2C5)^{1/2} = 10 \text{ ns}$. OA5 stage is a buffer.

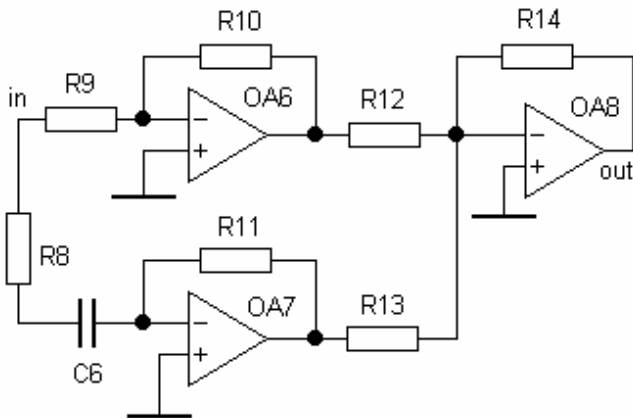


Fig. 13. First-order Taylor predictor. $C6 = 10 \text{ pF}$, $R8 = 10 \Omega$, $R9 = R10 = R11 = R12 = R13 = R14 = 1 \text{ k}\Omega$. Prediction time $T_{pred} \approx R11C6 = 10 \text{ ns}$.

Simulation of the overall analogue circuit has been performed using the 'Electronic Workbench Professional' simulator, based on the PSPICE software. The simulation results presented in Fig. 14 through Fig. 16 are in qualitative agreement with the numerical results of Section III obtained from a simplified mathematical model.

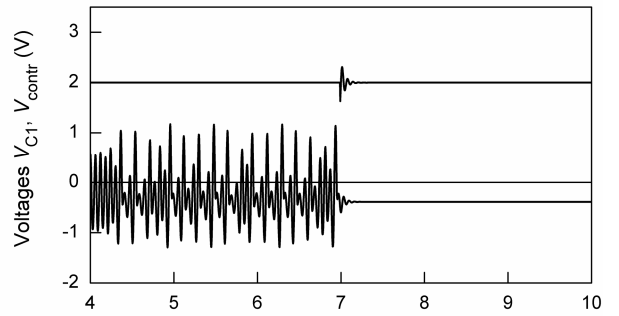


Fig. 14. PSPICE simulation results of the circuit in Fig. 9. Lower trace is $V_{out} = V_{C1}(t)$, the voltage across capacitor C1. Upper trace is the control signal $V_{contr}(t)$; it is shifted up by 2V for clarity. Switch is closed at $t = 7 \mu\text{s}$.

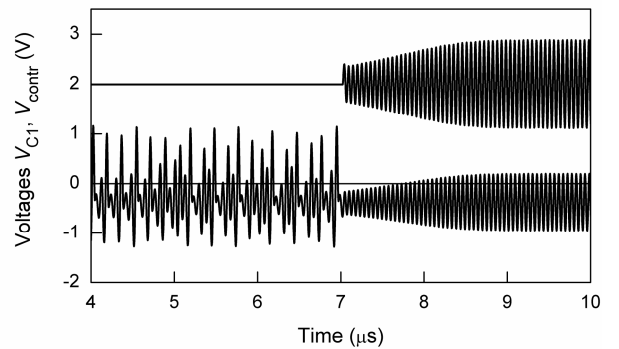


Fig. 15. PSPICE simulation results of the circuit in Fig. 9 with RC latency unit in Fig. 11. Signals, parameters and layouts are the same as in Fig. 14.

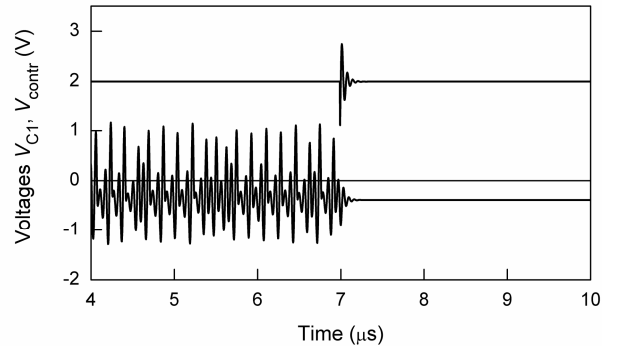


Fig. 16. PSPICE simulation results of the circuit in Fig. 9 with RC latency unit in Fig. 11 and predictor in Fig. 13. Signals, parameters and layouts are the same as in Fig. 14.

V. HARDWARE EXPERIMENTS

Practical circuit diagram is sketched in Fig. 17. Experiments for simplicity have been performed at lower frequencies, than simulated in Section IV, namely in the kilohertz range. Correspondingly, the L1C1C2 tank parameters of the oscillator in Fig. 9, the circuit parameters of the RC and the RLC latency units in Fig. 11 and Fig. 12, and the R11C6 value of the Taylor predictor in Fig. 13 have

been rescaled to larger values. Moreover, in the case of the specific oscillator considered in this paper the control loop can be simplified. The signal for control can be taken, alternatively to Fig. 9, not from the differential amplifier DIFF, but from the output of the OA1. The point is, that the output voltage of the OA1 is proportional to the voltage drop V_R across the resistor R, which is proportional to the current I_{L1} through the inductor L1. The I_{L1} is proportional to the derivative of the voltage across C1 ($I_{L1} \propto dV_{C1}/dt$). Thus, a simpler controller can naturally replace the two-stage derivative controller in Fig. 10, specifically the noninvertible OA9 based amplifier (Fig. 17).

The effective feedback coefficient $k = \gamma_1 \gamma_2 \gamma_3 \approx 0.8$, where the open-loop gain $\gamma_1 = R2/R1 + 1 = 1.5$, the open-loop gain $\gamma_2 = R15/R16 + 1 = 1.1$ and the open-loop gain via the inverting input of the OA1 $\gamma_3 = R2/R1 = 0.5$. Circuitry of the electronic switch is not displayed for simplicity.

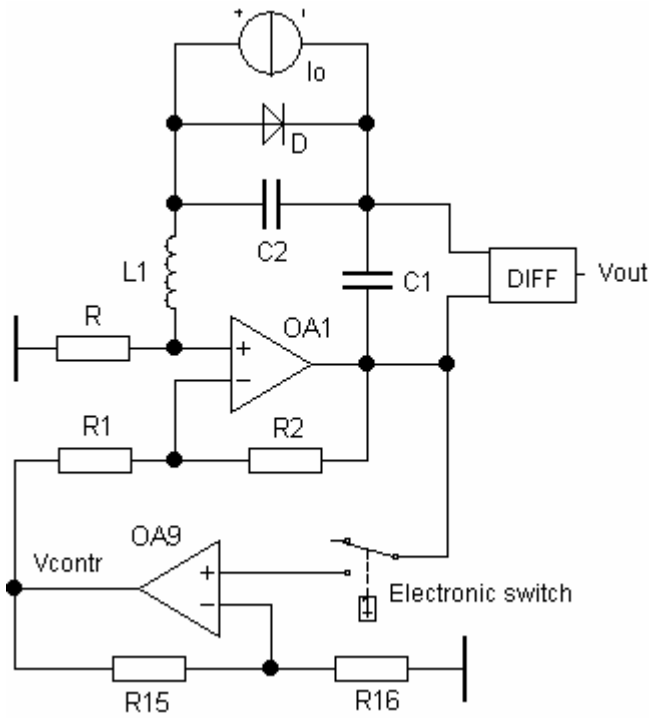


Fig. 17. Circuit diagram of the chaotic oscillator and the controller. D is an 1N4001 type general-purpose diode. DC bias $I_o = 10$ mA. DIFF is a differential amplifier; $V_{out} = V_{C1}$. $L1 = 20$ mH, $C1 = 1.5$ μ F; fundamental frequency $f^* = 1/2\pi(L1C1)^{1/2} \approx 1$ kHz, surge impedance $Z = (L1/C1)^{1/2} = 115$ Ω . $C2 = 100$ nF, $R = 115$ Ω , $R1 = 10$ k Ω , $R2 = 5.1$ k Ω , $R15 = 1$ k Ω , $R16 = 10$ k Ω ,

Hardware experimental snapshots of the output signals $V_{C1}(t)$ and the control signals $V_{contr}(t)$ shown in Fig. 18 through Fig. 20 are in a good agreement, both with the numerical solutions of equations (3) and with the PSPICE simulation results. They include all the main features, namely fast convergence to the stabilized steady state in the case of ideal controller (Fig 18), parasitic oscillations caused by latency (Fig. 19) and improved performance due to the insertion of the Taylor predictor (Fig. 20).

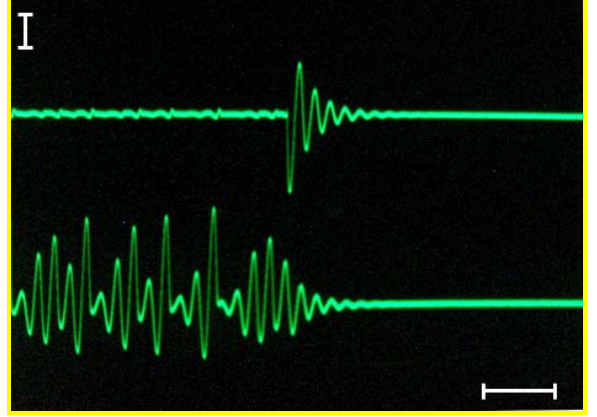


Fig. 18. Experimental results from the circuit in Fig. 17. Lower trace is $V_{C1}(t)$, the voltage across C1. Upper trace is the control signal $V_{contr}(t)$; it is shifted up for clarity. Horizontal scale: 5 ms/div., vertical scales: $V_{C1}(t) - 1$ V/div. $V_{contr}(t) - 0.5$ V/div.

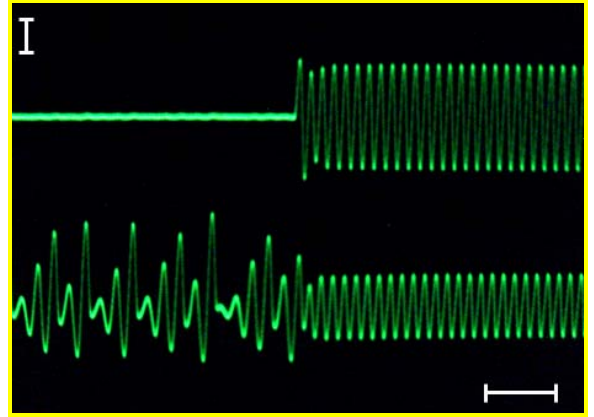


Fig. 19. Experimental results from the circuit in Fig. 17 but with additional RLC latency unit in Fig. 12 ($R7 = 1.6$ k Ω , $L2 = 200$ mH, $C5 = 100$ nF, $T_{del} = 200$ μ s). Signals and scales are the same as in Fig. 18.

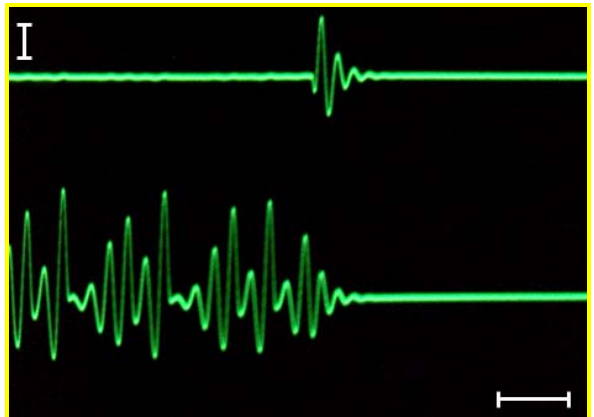


Fig. 20. Experimental results from the circuit in Fig. 17 but with additional RLC latency unit in Fig. 12 ($R7 = 1.6$ k Ω , $L2 = 200$ mH, $C5 = 100$ nF, $T_{del} = 200$ μ s) and the first-order Taylor predictor in Fig. 13 ($C6 = 20$ nF, $R8 = 100$ Ω , $R9 = R10 = R11 = R12 = R13 = R14 = 10$ k Ω , $T_{pred} \approx R11C6 = 200$ μ s). Signals and scales are the same as in Fig. 18.

VI. CONCLUSIONS

We have investigated the possibility to improve chaos controller by adding in the feedback loop an analogue Taylor predictor. Analysis shows that even for small latency times, e.g. 10 ns, the derivative control technique fails to stabilize USS of a chaotic system oscillating at the fundamental frequency $f^* \approx 16$ MHz (the mean period $1/f^*$ is about 60 ns). The time lag in the control loop of only 17% does not allow achieving stabilization. Moreover, it gives rise to high frequency parasitic oscillations at about 20 MHz. Meanwhile the inserted Taylor predictor compensates the latency effects and ensures perfect stabilization of the USS. An important result from a practical point of view is, that the prediction time should not exactly match the latency time. In addition, the order of the Taylor predictor should not necessarily equal the order of the circuit, causing the latency effect. The PSPICE and experimental results obtained for a realistic third-order chaotic circuit qualitatively confirm the findings from a simplified mathematical model.

In this paper we employed the simplest RC differentiator based first order Taylor predictor. Evidently, higher order Taylor predictors can be used. In addition, more sophisticated analogue predictors, like active filters based circuits [13, 14] and extended Taylor–Lagrange predictors [15] can be exploited.

Though the investigation has been performed for a specific system we expect similar results for other fast chaotic systems. The Taylor type predictors can be useful not only for the derivative control technique stabilizing USS, but also for various techniques designed to stabilize unstable periodic orbits, e.g. by the time-delayed feedback [21] and by second order resonant negative feedback [22] controllers.

ACKNOWLEDGMENT

The authors thank M. Meškauskas for performing some preliminary numerical simulations of equations (3) with an RLC type latency unit, similar to the RLC filter given by (9).

REFERENCES

- [1] *Handbook of Chaos Control*, H. G. Schuster, Ed. Berlin: Wiley, 1999.
- [2] *Exploiting chaotic properties of dynamical systems for their control: suppressing, enhancing, using chaos*, Theme Issue of *Phil. Trans. Roy. Soc.*, vol. A364, pp. 2267–2563, September 2006.
- [3] S. Bielawski, M. Bouazaoui, D. Derozier, and P. Glorieux, “Stabilization and characterization of unstable steady states in a laser,” *Phys. Rev.*, vol. A47, pp. 3276–3279, 1993.
- [4] G. A. Johnson and E. R. Hunt, “Derivative control of the steady state in Chua’s circuit driven in the chaotic region,” *IEEE Trans. Circ. Syst.*, vol. 40, pp. 833–834, 1993.
- [5] P. Parmananda, M.A. Rhode, G. A. Johnson, R. W. Rollins, H. D. Dewald, A. J. Maikworth, “Stabilization of unstable

steady state in an electrochemical system using derivative control,” *Phys. Rev.*, vol. E49, pp. 5007–5011, 1994.

- [6] A. Namajūnas, K. Pyragas, and A. Tamaševičius, “Stabilization of an unstable steady state in a Mackey-Glass system,” *Phys. Lett.*, vol. A204, pp. 255–262, 1995.
- [7] A. Namajūnas, K. Pyragas, and A. Tamaševičius, “Analog techniques for modeling and controlling the Mackey-Glass system,” *Int. J. Bif. Chaos*, vol. 7, pp. 957–962, 1997.
- [8] K. Pyragas, V. Pyragas, I. Z. Kiss, and J. L. Hudson, “Stabilizing and tracking unknown steady states of dynamical systems,” *Phys. Rev. Lett.*, vol. 89, pp. 244103–1–4, December 2002.
- [9] K. Pyragas, V. Pyragas, I. Z. Kiss, and J. L. Hudson, “Adaptive control of unknown unstable steady states of dynamical systems,” *Phys. Rev.*, vol. E70, pp. 026215–1–12, August 2004.
- [10] D. W. Sukow, M. E. Leich, D. J. Gauthier, and J. E. S. Socolar, “Controlling chaos in a fast diode resonator using extended time-delay autosynchronization: Experimental observations and theoretical analysis,” *Chaos*, vol. 7, pp. 560–576, 1997.
- [11] W. Just, D. Reckwerth, E. Reibold, and H. Benner, “Influence of control loop latency on time-delayed feedback control,” *Phys. Rev.*, vol. E59, pp. 2826–2829, March 1999.
- [12] P. Hövel and J. E. S. Socolar, “Stability domains for time-delay feedback control with latency,” *Phys. Rev.*, vol. E68, pp. 036206–1–7, September 2003.
- [13] M. Meškauskas, A. Tamaševičius, K. Pyragas, and G. Mykolaitis, “Signal prediction using active filters,” in *Proc. 2005 Int. Symp. on Nonlinear Theory and its Applications, NOLTA2005*, Bruges, Belgium, B. Motmans and T. Soma, Eds. Tokyo: IEICE, 2005, pp. 385–388.
- [14] M. Meškauskas, A. Tamaševičius, and K. Pyragas, “Analogue signal predictor: frequency-domain analysis,” *Int. J. Bif. Chaos*, vol. 17, October 2007, in press.
- [15] A. Tamaševičius, M. Meškauskas, and G. Mykolaitis, “Taylor analogue predictor supplemented with Lagrange remainder,” in *Proc. 14th Int. Workshop on Nonlinear Dynamics of Electronic Systems, NDES’2006*, Dijon, France, P. Marquié, Ed. Dijon: Université de Bourgogne, 2006, pp. 151–154.
- [16] R. D. Peters, “Spice modeling of the Vilnius chaotic oscillator,” [http:// physics.mercer.edu/hpage/vilnius.html](http://physics.mercer.edu/hpage/vilnius.html), 2005.
- [17] A. Tamaševičius, G. Mykolaitis, V. Pyragas, and K. Pyragas, “Simple chaotic oscillator for educational purposes,” *Eur J. Phys.*, vol. 26, pp. 61–63, January 2005.
- [18] V. Juškevičius, A. Tamaševičius, K. Pyragas, and G. Mykolaitis, “Third-order electrical circuit for courses on Nonlinear Dynamics and Chaos,” <http://www.pfi.lt/A.Tamasevicius/DynDays05.jpg>.
- [19] A. Tamaševičius, T. Pyragienė, K. Pyragas, S. Bumelienė, and M. Meškauskas, “Numerical treatment of educational chaos oscillator,” *Int. J. Bif. Chaos*, vol. 17, October 2007, in press.
- [20] G. Mykolaitis, A. Tamaševičius, S. Bumelienė, A. Namajūnas, K. Pyragas, V. Pyragas, “Application of ultrafast Schottky diodes to high megahertz chaotic oscillators,” *Acta Phys. Polon.*, vol. A107, pp. 365–368, February 2005.
- [21] K. Pyragas, “Delayed feedback control of chaos,” *Phil. Trans. Roy. Soc.*, vol. 364, pp. 2309–2334, September 2006.
- [22] A. Tamaševičius, E. Tamaševičiūtė, G. Mykolaitis, and S. Bumelienė, “Stabilization of unstable periodic orbit in chaotic Duffing–Holmes oscillator by second order resonant negative feedback,” *Lithuanian J. Phys.*, vol. 47, No. 3, in press, 2007.